# Negative refractive index response of weakly and strongly coupled optical metamaterials

Jiangfeng Zhou,[1] Thomas Koschny,[1,2] Maria Kafesaki,[2] and Costas M. Soukoulis[1,2]
[1]*Ames Laboratory and Department of Physics and Astronomy, Iowa State University, Ames, Iowa 50011, USA*
[2]*Department of Materials Science and Technology, University of Crete and Institute of Electronic Structure and Laser–Foundation for Research and Technology Hellas (FORTH), 71110 Heraklion, Crete, Greece*
(Received 11 May 2009; published 8 July 2009)

We present a detailed study of the retrieved optical parameters, electrical permittivity $\varepsilon$, magnetic permeability $\mu$, and refractive index $n$ of the coupled-fishnet metamaterial structures as a function of the separation between layers. For the weak-coupling case, the retrieved parameters are very close to the one-functional-layer results and converge relatively fast. For the strong-coupling case, the retrieved parameters are completely different from the one-unit fishnet results. We also demonstrate that the high value of the figure of merit [FOM=$|\mathrm{Re}(n)/\mathrm{Im}(n)|$] for the strongly coupled structures is due to the fact that the real part of the negative $n$ moves away from the maximum of the imaginary part of $n$ (close to the resonance), where the losses are high.

DOI: 10.1103/PhysRevB.80.035109 PACS number(s): 42.25.−p, 78.20.Ci, 41.20.Jb

## I. INTRODUCTION

Metamaterials are artificially engineered structures that have properties such as negative refractive index $n$, nonexistent in natural materials. The recent development of metamaterials[1] with negative $n$ confirms that structures can be fabricated and interpreted as having both a negative permittivity $\epsilon$ and a negative permeability $\mu$ simultaneously. Since the original microwave experiments for the demonstration of negative-index behavior in split ring resonators (SRRs) and wire structures, new designs have been introduced, such as fishnet, which have pushed the existence of the negative refraction at THz and optical wavelengths.[2–7] Most of the experiments with the fishnet structure measuring transmission $T$ and reflection $R$ use the retrieval procedure[8–11] to obtain the effective parameters $\epsilon$, $\mu$, and $n$. Although, the stacking of three-functional,[12] four-functional,[13] and ten-functional[14] layers, and the recently fabricated ten-functional-layer fishnets[7] (21 layers of silver and $MgF_2$) have been realized, they do not constitute a bulk metamaterial. Even the thickest fabricated fishnet structure[7] only has a total thickness of 830 nm, which is half of the wavelength ($\lambda=1700$ nm). Here, we report a detailed study of the weakly and strongly coupled fishnets to understand the origin of negative $n$, as well as the mechanism of low losses [i.e., high figure of merit (FOM)] for the weakly and strongly coupled fishnets. We also study the convergence of the retrieval parameters ($\epsilon$, $\mu$, and $n$) as the number of unit cells (layers) increases. For the weakly coupled structures, the convergence results for $n$ and FOM are close to the single unit cell. As expected, for the strongly coupled structures, hybridization is observed and the retrieval results for $n$ and FOM are completely different from the single unit cell. We demonstrate that the high value of FOM for the strongly coupled structure is due to the fact that the real part of negative $n$ moves away from the maximum of the imaginary part of $n$ (close to the resonance), where the losses are high.

The idea of left-handed materials, i.e., materials with both negative $\epsilon$ and negative $\mu$, where the electric field (**E**), magnetic field (**H**), and wave vector (**k**) form a left-handed coordinate system, was developed by Veselago[15] decades ago. However, it was only recently that such materials were investigated experimentally at high frequencies[2–7] and the field is driven by a wide range of new applications, such as ultrahigh-resolution imaging system,[16] cloaking devices,[17,18] and quantum levitation.[19] Realizing these applications, several goals must be achieved: three-dimensional rather than planar structure, isotropic design, and reduction of loss.

Most of the metamaterials exhibiting artificial magnetism,[13,14,20–22] and a negative refractive index $n$ at THz and optical frequencies[2–5,22] consist of only a functional layer. The number of actual layers $M=2\times N+1$, where $N$ is the number of functional layers. The first five-functional layer of SRRs operating at 6 THz was published[14] in 2005, and the occurrence of four layers of SRRs operating at 70 THz (Ref. 13) was published in 2008. The first three-functional layer of fishnets (seven layers of silver and $MgF_2$) operating at 200 THz was published[12] in 2007 and recently, a ten-functional layer of fishnets (21 layers of silver and $MgF_2$) operating at 200 THz was fabricated.[7] However, it is very important to study how the optical properties ($\epsilon$, $\mu$, and $n$) change as one increases the number of layers. How many layers are needed to achieve convergence of the optical properties and can one call this metamaterial bulk? How do optical properties behave as one changes the distance between two neighboring fishnets? If the distance is small, we have a strong-coupling case and one achieves the photonic-crystal limits. The convergence of optical properties is slow, and more importantly, it does not converge to the isolated fishnet case. What is the mechanism for negative $n$ in the strong-coupling limit?

In this paper, we present a detailed study of the retrieved optical parameters $\epsilon$, $\mu$, and $n$ of the single fishnet metamaterial structures as a function of the size of the unit cell. We find that as the size of the unit cell decreases, the magnitude of the retrieved effective parameters increases. In order to understand the underlying physics of the coupled structures, we study the retrieved parameters of the coupled fishnets as a function of the distance between them. Finally, we study the convergence of the retrieved parameters as the number of the unit cell increases for the weakly and strongly coupled structures. For the weakly coupling case, the retrieved parameters are very close to the one-functional-layer results and converge relatively fast. For the strong-coupling case, the re-

 

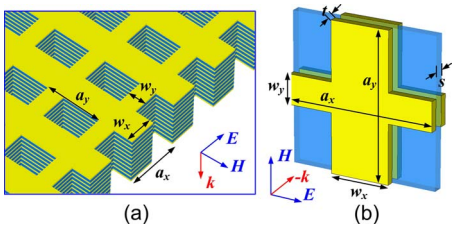


FIG. 1. (Color online) (a) Schematic of a fishnet structure with 11 metallic layers, (b) a single unit cell with geometric parameters marked on it.

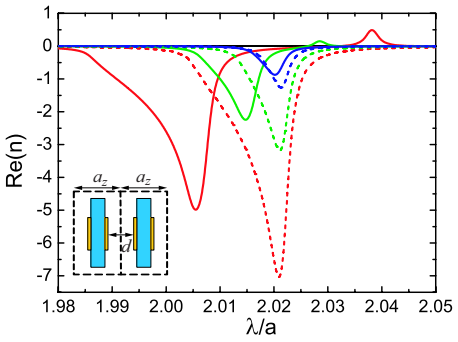


FIG. 2. (Color online) Retrieved real part of refractive index $n$ from simulated data using unit-cell size in the propagation direction $a_z=a/15$ (red), $a_z=2a/15$ (green), and $a_z=4a/15$ (blue). Both one-layer (dashed) and two-layer (solid) results are shown. The distances between two unit cells are $d=a_z-(2t+s)=0.04a$, $0.11a$, and $0.24a$, respectively. The other geometric parameters are given by $a_x=a_y=a$, $w_x=4a/15$, $w_y=3a/5$, $s=a/60$, $t=a/300$, and the dielectric constant of the spacer is $\epsilon_r=5$.

trieved parameters are completely different from the one-unit fishnet results. The strong-coupling case explains the recently observed negative refractive index in the 21-layer fishnet structure,[7] especially the high FOM, due to the periodicity effects, as will be shown below.

## II. WEAKLY AND STRONGLY COUPLED FISHNETS

In Fig. 1, we present a schematic graph of the unit cell of the fishnet structure. The size of the unit cell along the propagation direction is $a_z$. $a_z$ is larger than the sum of the thickness of the metallic and the dielectric layers $2t+s$, where $t$ and $s$ are the thicknesses of the metal and the dielectric layers, respectively. Notice that the propagation direction is perpendicular to the plane of the fishnet.

In most of the experiments measuring the $T$ and $R$ of the fishnet structure,[2–6,22] there is only one layer of the sample measured. In this case, the unit-cell size along the propagation direction $a_z$ is undefined. We have shown[23] that, as $a_z$ decreases, the magnitude of the retrieved parameters increases. It is well known from electronic systems that the monolayer of a surface can exhibit different properties from the bulk (many layers). Therefore, it is very important to systematically study whether the optical parameters of a single layer really correspond to the many-layer system. We will study the weak-coupling and strong-coupling limits of the two-layer fishnet structure.

Figure 2 shows the real part of the effective refractive index $\mathrm{Re}(n)$ as a function of $\lambda/a$ for one layer and two layers of the fishnet structure described in Fig. 1, with different distances between the unit cells. Notice the normalized resonance wavelength $\lambda_m/a \approx 2.02$, i.e., wavelength with maximum $|\mathrm{Re}(n)|$ for one layer shifts only slightly when the size of the unit cell increases but the magnitude of $|\mathrm{Re}(n)|$ decreases dramatically. For the two layers, when the distance $d$ between them is large ($d/a=0.24$, blue solid curve), the coupling between the two layers is weak and, therefore, the refractive index $\mathrm{Re}(n)$ approaches the one-layer simulation results. When the distance between the two layers becomes smaller ($d/a=0.04$, red solid curve) and the coupling becomes stronger, hybridization takes place and two resonance modes exist, one at $\lambda/2=2.005$, which gives $\mathrm{Re}(n)<0$, and one at 2.040, which has $\mathrm{Re}(n)>0$. The difference in value of the two resonance frequencies becomes larger as the distance between them decreases. Similar hybridization behavior was reported in a study of acoustic metamaterials.[24] Another very important issue is how fast the optical retrieval properties ($\epsilon$, $\mu$, and $n$) converge as the number of unit cells increases. We will present results for two cases, one for the weakly coupled fishnets.

The only design that gave negative $n$ at THz and optical frequencies is the so-called "double-fishnet" structure, which consists of a pair of metal fishnets separated by a dielectric spacer.[2–7] For the incident polarization shown in Fig. 1, the thin metallic wires along the $x$ axis, parallel to the incident electric field **E**, excite the plasmonic response and produce negative permittivity $\epsilon$ up to the plasma frequency. Negative $\mu$ is obtained from the wires along the $y$ axis, parallel to the incident magnetic field **H**. At the magnetic-resonance frequency, the two parallel bars sustain antiparallel currents (along $x$ axis), providing a magnetic field $\mathbf{B}'$ mainly between the plates and directly opposite to the external magnetic field **H**. The electric field, because of the opposite charges accumulated at the ends of the two metallic bars, is expected to be confined within the space between the plates and near the end points. Indeed, obtained simulations confirm this picture.

In Fig. 3, we present the retrieved results for the effective refractive index $\mathrm{Re}(n)$ as a function of $\lambda$ for different numbers of functional layers ($N=1$, 2, 3, 4, and 5) for weakly coupled fishnets system. The parameters are exactly the same as in the strongly coupled case that will be discussed below but the spacing between the functional layers is $d=90$ nm. As can be seen in Fig. 3, the retrieved results for $\mathrm{Re}(n)$ converge very fast ($N=2$) and the convergence results agree with the results of the one-functional layer of the fishnet.

When the fishnets strongly interact, it is not clear what the mechanism is for giving negative $n$. As discussed in Fig. 2, the isolated fishnet resonance frequency hybridizes into two different modes. The antisymmetric mode gives weak resonance with $n \approx 0$ while the symmetric mode gives a strong resonance with a strong negative $n$. In Fig. 4, we present results for the retrieved $\mathrm{Re}(n)$ for different number of layers (3–27) for the recently fabricated[7] negative-index structure. Notice that, in the low wavelength limit (between 1200 and 2100 nm), convergence of $n$ is obtained and agrees with experimental results of Ref. 7. In the high wavelength limit

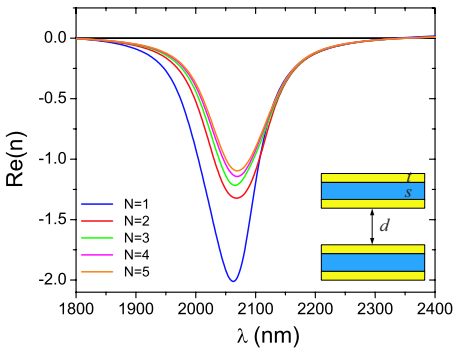


FIG. 3. (Color online) Retrieved real part of effective refractive index Re($n$) for one to five functional layers of the fishnet structure. The geometric parameters are $a_x=a_y=860$ nm, $w_x=565$ nm, $w_y=265$ nm, $s=50$ nm, $t=30$ nm, $d=90$ nm, and the spacer is made from $MgF_2$ with the dielectric constant $\epsilon_r=1.9$. The functional layers are separated by vacuum layers with thickness $d$ as shown in the inset.

($\lambda>2200$ nm), Re($n$) is zero and Im($n$) is much larger than Re($n$), exhibiting that the metallic behavior and the transmission is equal to zero. This metallic behavior can also be seen in the transmission $T$ (see the supplementary material) for the many-layer structure. Above 2200 nm, $T$ is low and behaves as a metal while for $\lambda<2000$ nm, $T$ is relatively large ($\sim$0.8) and has Fabry-Perot resonance structure. The $|\mathrm{Re}(n)|$ shown in Fig. 4 converges between 1200 and 2200 nm to a finite value (positive for wavelengths less than 1500 nm and negative for $1500<2200$ nm). For $\lambda>2200$ nm, $|\mathrm{Re}(n)|$ is zero and $|\mathrm{Im}(n)|$ is large of the order of three, and as expected for large wavelengths, this strongly coupled metamaterial behaves as a metal. In addition, in Fig. 4, the three-layer structure (the single fishnet structure) gives results completely different from those for the strongly coupled fishnets. These single fishnet results agree with those presented in Fig. 3. Another important quantity is the FOM, which can be defined in two different ways. The usual definition is $\mathrm{FOM}=|\mathrm{Re}(n)/\mathrm{Im}(n)|$ and the experimental definition of Im($n$) is given by $\mathrm{Im}(n)=(\lambda/4\pi d)\ln[(1-|R|)/|T|]$, where $\lambda$,

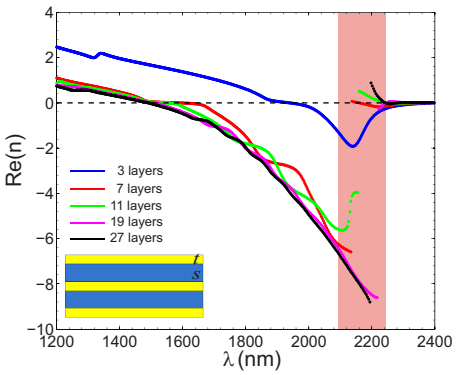


FIG. 4. (Color online) The retrieved real part of $n$ for 3-layer, 7-layer, 11-layer, 19-layer, and 27-layer strongly coupled fishnet structures. The geometric parameters are $a_x=a_y=860$ nm, $w_x=565$ nm, $w_y=265$ nm, $s=50$ nm, and $t=30$ nm, and the spacer is made from $MgF_2$ with the dielectric constant $\epsilon_r=1.9$. The shadow region shows where the discontinuity happens.

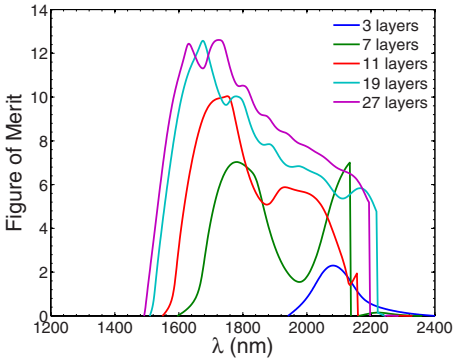


FIG. 5. (Color online) The FOM of $\mathrm{Re}(n)<0$ region for 3-layer, 7-layer, 11-layer, 19-layer, and 27-layer strongly coupled fishnet structures. The FOM is calculated by $\mathrm{FOM}=|\mathrm{Re}(n)/\mathrm{Im}(n)|$, where Re($n$) is obtained by a retrieval procedure and Im($n$) is calculated by $\mathrm{Im}(n)=(\lambda/4\pi d)\ln[(1-|R|)/|T|]$.

$d$, $R$, and $T$ are the wavelength, sample thickness, reflectance, and transmittance, respectively.

## III. FIGURE OF MERIT CALCULATIONS

In Fig. 5, we present the results of the FOM as a function of wavelength for different numbers of layers. For the one-unit-cell fishnet (three layers), the FOM is really small (of the order of two) and is located at $\lambda=2100$ nm, the resonance frequency of the single fishnet structure. As the number of layers increases, the FOM increases and finally saturates to a constant value of the order of ten. This behavior of the FOM for the strongly coupled fishnets is completely different for the weakly coupled fishnets, where the FOM does not change dramatically[3] as one uses more unit cells. Why is the FOM in the strongly coupled fishnets so much different from the single fishnet? It has been argued[7,25] that the FOM is larger because of the strong coupling between the neighboring layers, which provides destructive interference of the antisymmetric currents across the metal film and effectively cancels the current in the center of the film, and, therefore, reduces the losses. We have systematically studied the current density for different numbers of strongly coupled fishnet structures. For the single fishnet structure, the current density is along opposite directions in the two metallic bars. This is the typical behavior of negative-index materials. When the number of layers increases, the current density is more complicated, and there is no clear physical explanation why one obtains negative $n$ and why the FOM is so large.

In Fig. 6, we present the current density along the $x$ axis (or **E** direction, as shown in Fig. 1) $J_x$ of the antisymmetric and symmetric modes for the seven-layer (four metallic layers and three dielectric layers) strongly coupled structure. For the antisymmetric mode [as shown in Fig. 6(a)], two double fishnets are formed by the first and second silver layers, and by the third and fourth silver layers. The induced current inside two double fishnets excites the magnetic fields $\mathbf{B}'$ along the same direction. However, the second and third silver layers also form a double fishnet, which excites the magnetic fields in the opposite direction. Therefore, the ex-

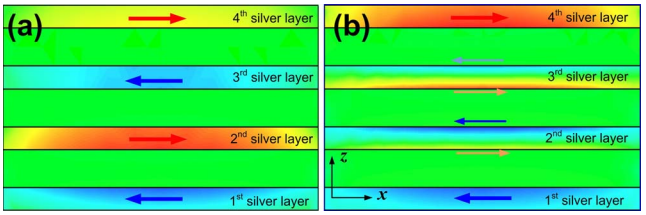


FIG. 6. (Color online) (a) The current-density distribution for a seven-layer strongly coupled fishnet at wavelength $\lambda=2230$ nm (antisymmetric mode) with $\mathrm{Re}(n)=-0.17$. (b) The current-density distribution for a seven-layer strongly coupled fishnet at wavelength $\lambda=1859$ nm (symmetric mode) with $\mathrm{Re}(n)=-2.5$. The cross-section is perpendicular to the $y$ axis (i.e., incident magnetic filed, **H**, direction). The color shows the current density in $x$ direction $J_x$, with the red and blue being the positive maximum and negative maximum of $J_x$, respectively. The arrows show the direction of current density inside the silver layers schematically.

cited magnetic fields $\mathbf{B}'$ are always antiparallel in the space between neighboring silver layers and cancel each other. This explains the observation of a weak resonance with nearly zero $n$. For the symmetric mode shown in Fig. 6(b), the first and fourth silver layers have current density along opposite directions and are almost uniform for all the metallic thickness of 30 nm silver layers. In the second and third silver layers, the current density is no longer uniform in all thicknesses of the silver layers. Instead, the current flows along opposite directions on the two surfaces of each layer. Due to the antiparallel current on the surfaces of the second and third silver layers, the induced magnetic field $\mathbf{B}'$, in the space between neighboring silver layers, is always parallel to each other. As a consequence, the seven-layer structure can be viewed as three-cascade double-fishnet structures, with the induced magnetic fields $\mathbf{B}'$ along the same direction. Therefore, the symmetric mode results in a strong resonance with large negative $n$. Our detailed numerical work, shown in Figs. 4 and 6, explains very well why we obtain very low $n\approx 0$ at $\lambda=2230$ nm and why we obtain high negative $n=-2.5$ at $\lambda=1859$ nm. However, it is not clear that if this

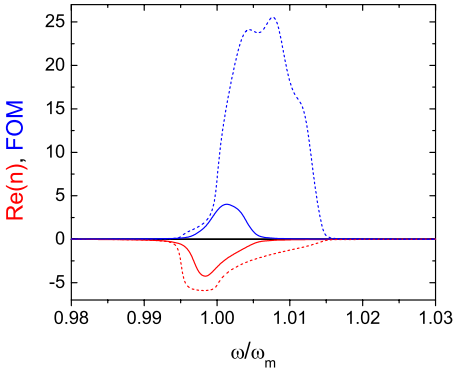


FIG. 7. (Color online) The real parts of refractive index (red), $\mathrm{Re}(n)$, and the FOM (blue) for the single-layer fishnet structures with spacer thickness $s=0.025a$ (solid curves) and $0.1a$ (dashed curves), respectively. The other geometric parameters are given by $a_x=a_y=a$, $w_x=2a/5$, $w_y=a/3$, $t=a/300$, and the dielectric constant of the spacer is $\epsilon_r=5$.

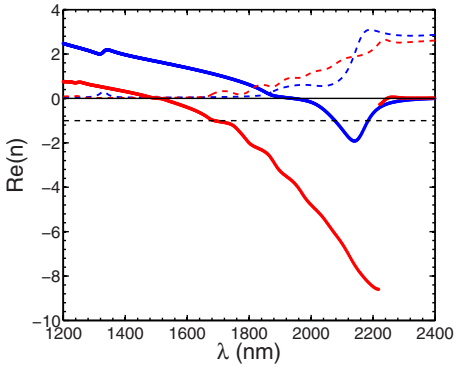


FIG. 8. (Color online) The real (solid curves) and imaginary (dashed curves) parts of refractive index $\mathrm{Re}(n)$ and $\mathrm{Im}(n)$ for the 3-layer (blue) and 19-layer (red) fishnet structures. The black dashed line shows the position where $\mathrm{Re}(n)=-1$.

current-density distribution is responsible for the high FOM shown in Fig. 5.

The reason that the single unit cell (metal-dielectric-metal) has low FOM or high losses is due to its resonance structure. One way to increase the FOM, which is the ratio of $|\mathrm{Re}(n)/\mathrm{Im}(n)|$, is to move away from the resonance frequency, where $\mathrm{Im}(n)$ is large and, therefore, the FOM can increase dramatically. This can be accomplished in both the weakly and strongly coupled fishnets by introducing periodicity effects. For the single-unit-cell fishnet, we can increase the size of the spacing layer and one can see from Fig. 7 that with a thicker spacing layer $s=0.1a$, $\mathrm{Re}(n)$ reaches the Brillouin zone, and the $\mathrm{Re}(n)<0$ region is extended to the area where $\mathrm{Im}(n)\approx 0$, so the FOM reaches a large value of 25.

In Fig. 8, we present both the real and the imaginary parts of the refractive index, $\mathrm{Re}(n)$ and $\mathrm{Im}(n)$, for the 3-layer and the 19-layer fishnet structures. For the three-layer structure (the single layer of double fishnet), $\mathrm{Re}(n)$ has a smooth resonance curve (blue solid). The bandwidth of the $\mathrm{Re}(n)<0$ region is relatively narrow and close to the peak of $\mathrm{Im}(n)$ (blue dashed) so the FOM is very small (as shown in Fig. 5). For the 19-layer fishnets, the $\mathrm{Re}(n)$ curve (red solid) does not have the resonance behavior expected for a single functional layer but it is very broad and has structure, which is due to periodicity effects.[9] Notice that for the 19-layer structure, $\mathrm{Re}(n)=-1$ at $\lambda=1688$ nm and $\mathrm{Im}(n)$ is 0.14 so the FOM is of the order of ten. However, for the three-layer structure, $\mathrm{Re}(n)=-1$ at $\lambda=2075$ and 2185 nm, and the $\mathrm{Im}(n)$ is 0.44 and 1.43, respectively, so the FOM is of the order of one. Therefore, due to the distortion of $\mathrm{Re}(n)$ caused by the periodicity effects, the FOM of the fishnet structure increases dramatically as the number of layers increases.

## IV. CONCLUSIONS

We have made a systematic study of the weakly and strongly coupled fishnets to understand the origin of negative $n$, as well as the origin of losses and the large value of the FOM for the strongly coupled fishnets. We studied the size dependence of the retrieved parameters ($\epsilon$, $\mu$, and $n$) of the weakly and strongly coupled fishnet structures. For both

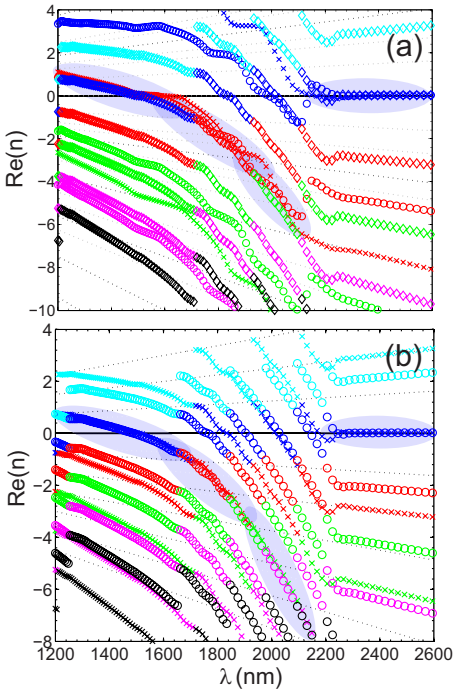


FIG. 9. (Color online) Branches of the refractive index Re($n$) with $m=1$ (cyan), 0 (blue), −1 (red), −2 (green), −3 (magenta), and −4 (black). The cross, circle, and diamond symbols in (a) represent Re($n$) for 7-layer, 11-layer, and 19-layer strongly coupled fishnet structures, respectively. The cross and circular symbols in (b) represent the 19-layer and 27-layer strongly coupled fishnet structures, respectively. The shadow region shows where different branches overlap for 7-layer, 11-layer, 19-layer, and 27-layer fishnet structures. The gray-dotted lines show the branch boundaries that are given by $m\pi/kL$.

cases, we have found that the retrieved parameters have a strong resonance behavior as the size of the unit cell decreases. We have also studied the convergence of the retrieved parameters as the number of unit cells (layers) increases. For the weakly coupled fishnet structures, we have found that the convergence results are relatively close to the single unit cell. Also, the converged FOM for the weakly coupled fishnet is the same order of magnitude as the single fishnet. For the strongly coupled fishnet structures, we have demonstrated that hybridization happens and we have two resonance modes. The antisymmetric resonance mode gives a strong negative $n$. As more unit cells or layers are added, the convergence of the retrieval parameters is completely different from the single fishnet results and the FOM is much larger than the single fishnet. We have demonstrated that the large FOM for the strongly coupled fishnet is due to the periodicity effects.

## ACKNOWLEDGMENTS

We thank M. Wegener for useful discussions. Work at Ames Laboratory was supported by the Department of Energy (Basic Energy Sciences) under Contract No. DE-AC02-07CH11358. This work was partially supported by the Department of Navy, Office of Naval Research (Award No. N00014-07-1-0359), European Community FET project PHOME (Contract No. 213390), and AFOSR under MURI Grant No. FA 9550-06-1-0337.

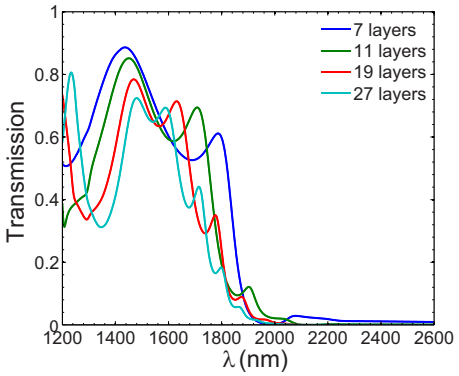


FIG. 10. (Color online) Transmission spectra for 7-layer, 11-layer, 19-layer, and 27-layer strongly coupled fishnet systems.

## APPENDIX: EFFECTIVE PARAMETER RETRIEVAL FOR STRONGLY COUPLED FISHNETS

The effective retrieved parameter ($\epsilon$, $\mu$, $n$, and $z$) of single layer and many layers of metamaterial can be obtained from the transmission $T$ and reflection coefficient $R$. There is a need for $T$ and $R$ to be inverted. As was discussed in detail in the literature,[10–13] one can invert $T$ and $R$

$$z(\omega) = \pm \sqrt{\frac{(1+R)^2 - T^2}{(1-R)^2 + T^2}}, \tag{A1}$$

$$n(\omega) = \pm \frac{1}{kL}\arccos\left(\frac{1-R^2+T^2}{2T}\right) + m\frac{2\pi}{kL}, \tag{A2}$$

where $L$ is the width of the homogeneous slab and $m = \pm 1, \pm 2, \ldots$. Note that both functions, $z(\omega)$ and $n(\omega)$, have multiple branches. The correct branch for $z(\omega)$ is chosen by imposing the physical requirement $\mathrm{Re}(z) \geq 0$, which is due to causality. The problem with the different branches of Re($n$) can be solved by considering different lengths for $L$ and one has to choose the branches that overlap. Especially if one has many layers, then many branches exist and one has to be very careful to select the correct ones. For the strongly coupled layers for which the results were presented in Fig. 4, we would like to discuss how these branches were selected. The unit-cell size is called $d_0$ and it consists of metal-dielectric-metal, and its width is $d_0 = 160$ nm.

In Fig. 9(a), we plot the branches and the retrieval results for 7 layers (width$=2d_0$), 11 layers (width$=3d_0$), and 19 layers (width$=5d_0$). Notice that the solutions for Re($n$) overlap between 1200 nm and all the way to 2200 nm, and give negative values of Re($n$). For $\lambda > 2200$ nm, $\mathrm{Re}(n) \approx 0$ and converges, and the $\mathrm{Im}(n) \approx 3$ in this region. Therefore, for $\lambda > 2200$ nm, the strongly coupled optical materials behave as a metal. In Fig. 9(b), we plot the branches and the retrieved result for 19 layers (width$=5d_0$) and 27 layers (width$=7d_0$), and one can see clearly that the convergence is

much better for these larger systems. So we have solutions consisting of two discontinued regions for $\mathrm{Re}(n)$, $\mathrm{Re}(n) \approx 0$ for $\lambda > 2200$ nm, and negative for $1500\ \mathrm{nm} < \lambda < 2200$ nm.

In Fig. 10, we present the results for transmission $T$ versus wavelength. Notice that for $\lambda > 2200$ nm, $T \approx 0$, which is a metallic behavior and this is the reason that $\mathrm{Re}(n) \approx 0$ and $\mathrm{Im}(n) \approx 3$ for $\lambda > 2200$ nm.


[1] C. M. Soukoulis, M. Kafesaki, and E. N. Economou, Adv. Mater. **18**, 1941 (2006); C. M. Soukoulis, S. Linden, and M. Wegener, Science **315**, 47 (2007); V. M. Shalaev, Nat. Photonics **1**, 41 (2007).

[2] S. Zhang, W. Fan, N. C. Panoiu, K. J. Malloy, R. M. Osgood, and S. R. J. Brueck, Phys. Rev. Lett. **95**, 137404 (2005).

[3] G. Dolling, C. Enkrich, M. Wegener, C. M. Soukoulis, and S. Linden, Opt. Lett. **31**, 1800 (2006).

[4] G. Dolling, C. Enkrich, M. Wegener, C. M. Soukoulis, and S. Linden, Science **312**, 892 (2006).

[5] U. K. Chettiar, A. V. Kildishev, H. K. Yuan, W. Cai, S. Xiao, V. P. Drachev, and V. M. Shalaev, Opt. Lett. **32**, 1671 (2007).

[6] M. Kafesaki, I. Tsiapa, N. Katsarakis, T. Koschny, C. M. Soukoulis, and E. N. Economou, Phys. Rev. B **75**, 235114 (2007).

[7] J. Valentine, S. Zhang, T. Zentgraf, E. Ulin-Avila, D. A. Genov, G. Bartal, and X. Zhang, Nature (London) **455**, 376 (2008).

[8] D. R. Smith, S. Schultz, P. Markos, and C. M. Soukoulis, Phys. Rev. B **65**, 195104 (2002).

[9] T. Koschny, P. Markos, E. N. Economou, D. R. Smith, D. C. Vier, and C. M. Soukoulis, Phys. Rev. B **71**, 245105 (2005).

[10] D. R. Smith, D. C. Vier, T. Koschny, and C. M. Soukoulis, Phys. Rev. E **71**, 036617 (2005).

[11] X. D. Chen, T. M. Grzegorczyk, B. I. Wu, J. Pacheco, and J. A. Kong, Phys. Rev. E **70**, 016608 (2004).

[12] G. Dolling, M. Wegener, and S. Linden, Opt. Lett. **32**, 551 (2007).

[13] N. Liu, H. C. Guo, L. W. Fu, S. Kaiser, H. Schweizer, and H. Giessen, Nature Mater. **7**, 31 (2008).

[14] N. Katsarakis, G. Konstantinidis, A. Kostopoulos, R. Penciu, T. Gundogdu, M. Kafesaki, E. Economou, T. Koschny, and C. M. Soukoulis, Opt. Lett. **30**, 1348 (2005).

[15] V. G. Veselago, Sov. Phys. Usp. **10**, 509 (1968).

[16] X. Zhang and Z. W. Liu, Nature Mater. **7**, 435 (2008).

[17] J. B. Pendry, D. Schurig, and D. R. Smith, Science **312**, 1780 (2006).

[18] D. Schurig, J. J. Mock, B. J. Justice, S. A. Cummer, J. B. Pendry, A. F. Starr, and D. R. Smith, Science **314**, 977 (2006).

[19] U. Leonhardt and T. G. Philbin, New J. Phys. **9**, 254 (2007).

[20] T. J. Yen, W. J. Padilla, N. Fang, D. C. Vier, D. R. Smith, J. B. Pendry, D. N. Basov, and X. Zhang, Science **303**, 1494 (2004).

[21] S. Linden, C. Enkrich, M. Wegener, J. F. Zhou, T. Koschny, and C. M. Soukoulis, Science **306**, 1351 (2004).

[22] G. Dolling, C. Enkrich, M. Wegener, J. F. Zhou, and C. M. Soukoulis, Opt. Lett. **30**, 3198 (2005).

[23] J. F. Zhou, T. Koschny, M. Kafesaki, and C. M. Soukoulis, Photonics Nanostruct. Fundam. Appl. **6**, 96 (2008).

[24] S. Guenneau, A. B. Movchan, and S. A. Ramakrishna, New J. Phys. **9**, 399 (2007).

[25] T. Li, H. Liu, F. M. Wang, Z. G. Dong, S. N. Zhu, and X. Zhang, Opt. Express **14**, 11155 (2006).